IFMIF: Overview of the Validation Activities

J. Knaster[1], F. Arbeiter[2], P. Cara[3], P. Favuzza[4,] F. Groeschel[1], R. Heidinger[3], A. Ibarra[5], H. Matsumoto[1], A. Mosnier[3], M. Sugimoto[6], H. Suzuki[6], E. Wakai[6]

[1]IFMIF/EVEDA Project Team, Rokkasho, Japan; [2]KIT, Karlsruhe, Germany; [3]F4E, Garching, Germany; [4]ENEA, Brasimone, Italy; [5]CIEMAT, Madrid, Spain; [6]JAEA, Rokkasho, Japan.

E-mail contact of corresponding author: juan.knaster@ifmif.org

Abstract. The Engineering Validation and Engineering Design Activities (EVEDA) for the International Fusion Materials Irradiation Facility (IFMIF), an international collaboration under the Broader Approach Agreement between Japan Government and EURATOM, aims at allowing a rapid construction phase of IFMIF in due time with an understanding of cost involved. The three main facilities of IFMIF: 1) the Accelerator facility, 2) the Target facility and 3) the Test facility are the subject of validation activities that include the construction of either full scale prototypes or smartly devised scaled down facilities that will allow a straightforward extrapolation to IFMIF needs. By July 2013, the engineering design activities of IFMIF matured with the delivery of an Intermediate IFMIF Engineering Design Report (IIEDR) supported by experimental results. The installation of a Linac of 1.125 MW (125 mA and 9 MeV) of deuterons started in March 2013 in Rokkasho (Japan). The world largest liquid Li test loop is running in Oarai (Japan) with an ambitious experimental programme for the years ahead. A full scale High Flux Test Module that will house ~1000 small specimens developed jointly in Europe and Japan for the Fusion programme has been constructed by KIT (Karlsruhe) together with its He gas cooling loop. A full scale Medium Flux Test Module to carry out on-line creep measurement has been constructed by CRPP (Villigen).

1. Introduction

In DEMO like in future fusion power plants, the deuterium-tritium nuclear fusion reactions will generate a large quantity of 14.1 MeV neutrons that will collide with the materials of the reactor vessel. The first wall, a combination of layers of different materials that aims to maximize the conversion of neutrons into thermal energy and breed tritium will be critically exposed. Understanding the degradation of the mechanical properties throughout the reactor operational life is a key parameter to allow the design and eventual facility licensing by the corresponding nuclear authorities.

Inelastic collisions of neutrons with the nuclei in the structural materials over the threshold incident energy of around 3 MeV will transmute heavy nuclei, which can decay releasing p^+ and α-particles. In turn, the elastic collisions are measured by NRT displacements per atom (NRT dpa) [1] with a cross section inversely proportional to the average displacement energy threshold for production of a Frenkel vacancy-interstitial atom defect pair in the material. Not all the materials will present the same NRT dpa under same neutrons bombardment, neither will all areas inside the reactor vessel undergo the same flux and spectrum of neutrons. In addition, NRT dpa do not take into account the time-evolution of radiation damage in the materials, such as recombination, migration, and coalescence of radiation defects, and in this sense they represent an atom-based approximate measure of the irradiation exposure of the material to the fusion neutrons. The generation of He and H from transmuted elements together with displacement effects in the materials lattice under fusion-like neutron bombardement has inherent uncertainties on the effects on mechanical and physical properties that can only be overcome through testing in as close as possible conditions [2].

IFMIF, the International Fusion Materials Irradiation Facility, will generate a neutron flux with a peak at around 14 MeV by (d,Li) stripping reactions thanks to two parallel deuteron accelerators colliding in a liquid Li screen with a footprint of 20 cm x 5 cm. The energy of the beam (40 MeV) and the current of the parallel accelerators (2 x 125 mA) have been tuned to maximize the neutrons flux (10^{18} $m^{-2}s^{-1}$) to get irradiation conditions comparable to those in the first wall of a fusion reactor in a volume of 0.5 l that will house around 1000 small specimens [3]. This will allow the accurate determination of those properties considered critical (fatigue, fracture toughness, crack growth rate, creep and tensile stress) of suitable materials and allow the understanding of the degradation that will lead to design more radiation hard components.

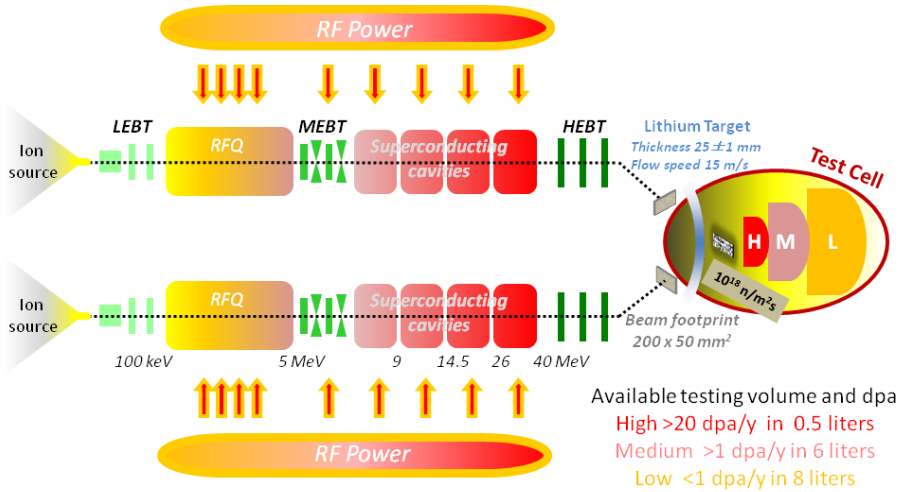

Figure 1. Schematic of IFMIF.

The purposed-designed reduced activation ferritic-martensitic steels (RAFM) present typically around 80% of its constituents presenting an average displacement energy (Wigner energy) of 40 eV that can reach over 15 dpa/year in a full power operation fusion reactor [4]. The accumulation of gas in the materials lattice is intimately related with neutron energy threshold at around 3 MeV; neutrons below these energies do not transmute the Fe nuclei and therefore gas is not efficiently generated. This is a major drawback for fusion materials testing in fission reactors as they present average n energies around 2 MeV. In turn, spallation sources present a neutron spectrum with long tails reaching the hundreds MeV range transmutation efficiency, especially for the lighter elements which have a high potential in deteriorating mechanical properties. A comparison of IFMIF with other available neutron sources has been performed [5], where it is explained how the spectrum that IFMIF provides, reproduces accurately fusion reactors spectrum with a flattop near the 14 MeV peak and at intermediate energies, while the closest available spallation sources, ESS and XADS, are one order of magnitude lower in flux in these critical range of energies.

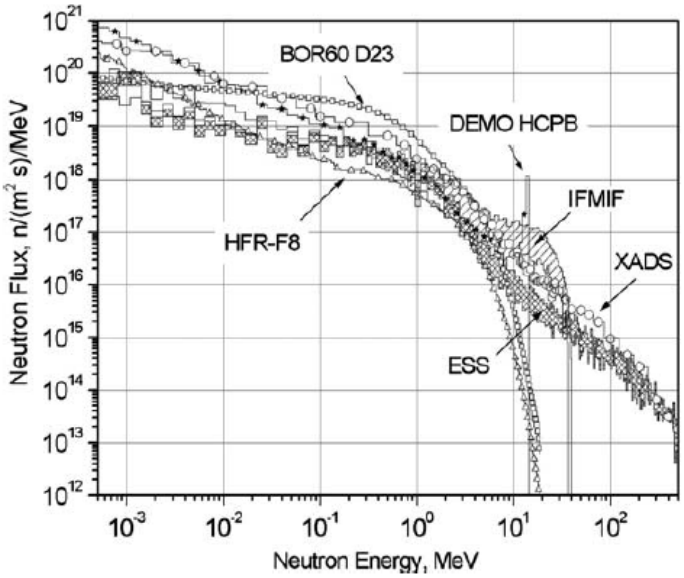

Figure 2. Neutron flux compared with the one DEMO will present in available and planned neutron sources including IFMIF [5]

IFMIF, presently in its Engineering Validation and Engineering Design Activities phase (IFMIF/EVEDA), started in 2007 under the framework of the Broader Approach (BA) Agreement between EURATOM and Japan, is entering into conclusive stages [6]. In July 2013, the engineering design of IFMIF have been completed with the delivery of an Intermediate IFMIF Engineering Design Report (IIEDR) supported by experimental results [7].

An overview of the validation activities already achieved is reported. Details of on-going validation activities will be provided.

2. IFMIF Validation Activities

The validation activities have been the subject of a successful Japan-Europe scientific collaboration [8,9]. In order to produce the experimental backing of the IFMIF Design during the EVEDA phase, 3 major prototypes have been designed and manufactured:

- an Accelerator Prototype (LIPAc) at Rokkasho, fully representative of the IFMIF low energy (9 MeV) accelerator (125 mA of D^+ beam in continuous wave) to be completed in June 2017 [10,11];
- a Lithium Test Loop (ELTL) at Oarai, integrating all elements of the IFMIF lithium target facility, already commissioned in February 2011 [12,13] complemented by corrosion experiments performed at the LIFUS6 lithium loop at Brasimone [14];
- the High Flux Test Module (different designs) [15,16] and its internals to be irradiated in a fission reactor [17] and tested in the helium loop HELOKA [18] complemented the Creep Fatigue Test Module [19] manufactured and tested in full scale at Villigen.

While this overview has to leave to the above cited papers the description of design and experimental details, also of the overall activities, the focus is given here to the outcome of the validation activities already achieved and still expected.

2.1 The Accelerator Facility Validation activities

The accelerator requirements of the Linear IFMIF Prototype Accelerator (LIPAc), in comparison with IFMIF, are given in the following synthetic table defining its main specifications:

TABLE I: MAIN PARAMETERS OF LIPA (COMPARED TO IFMIF ACCELERATORS)

Primary Parameters	**LIPAc**	**IFMIF**	**Units**
Number of Linacs	1	2	-
Duty factor	CW	CW	-
Ion type	D^+	D^+	-
Beam intensity on target	125	2 x 125	mA
Beam kinetic energy on target	9	40	MeV
Beam Power on target	1.125	2 x 5	MW
RF Frequency	175	175	MHz
Target material	Cu	Li	-
Total length	34.0	84.7	m
Injector length	5.0	5.0	m
RFQ length	9.8	9.8	m
MEBT length	2.3	2.3	m
SRF Linac length	4.6	22.4	m
Number of cryomodules	1	2 x 4	-
HEBT total length	9.6	45.0	m

The setting-up of the 1.125 MW Linac in Rokkasho, for which the first accelerator sub-systems provided by the European Home Team has arrived in March 2013, requires a well-coordinated integration and commissioning programme, due to the distributed nature of the deliveries (see figure 3):

- The accelerator components designed, manufactured and tested by European institutions (CEA, CIEMAT, INFN, SCK-CEN) are: Injector, Radio Frequency Quadrupole (RFQ), Medium and High Energy Beam Transport lines, Superconducting RF Linac, Beam Dump, 175 MHz RF Systems, Local Control Systems, Beam Instrumentation;

- The conventional facilities (building and main auxiliaries), the Central Control System, as well as the RFQ couplers, are provided by JAEA;

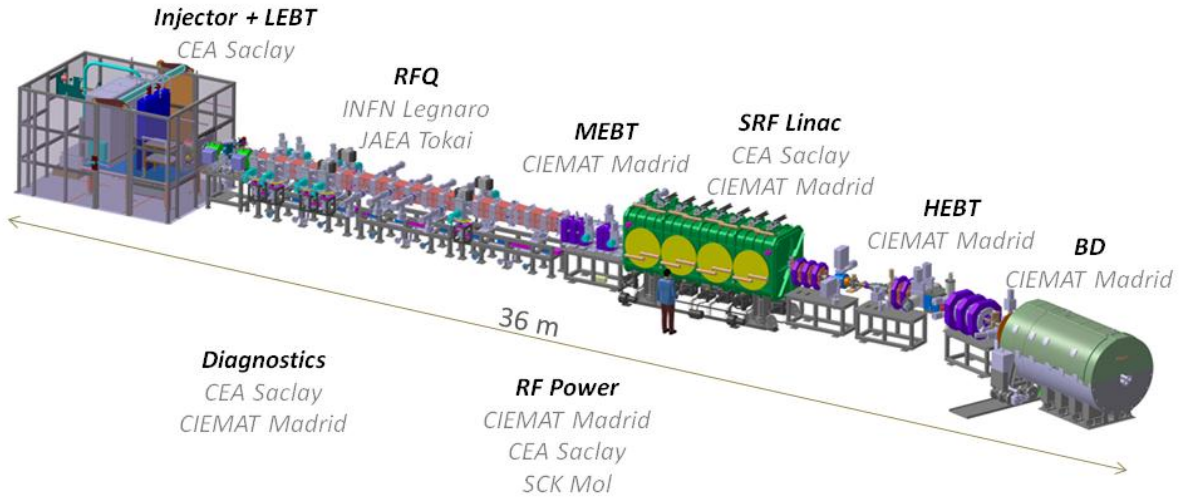

Figure 3. Layout of IFMIF accelerator validation facility with the indication of the different laboratory contributions

As an essential element of this programme, specific central databases, management systems and procedures is being implemented such as a documentation management system, an interface management system, assembly procedures and a 3D configuration management of the facility [20].

The LIPAc beam is generated by an injector (4.4) using an Electron Cyclotron Resonance (ECR) deuteron (D^+) source (4.4.1). After being properly focussed and filtered along the Low Energy Beam Transport (LEBT, 4.4.2) unit, the D+ beam is accelerated by two successive systems: a normal-conducting RFQ (4.5) and 8 superconducting Half-Wave Resonators (HWR) located within the SRF Linac (4.7) (see figure 4).

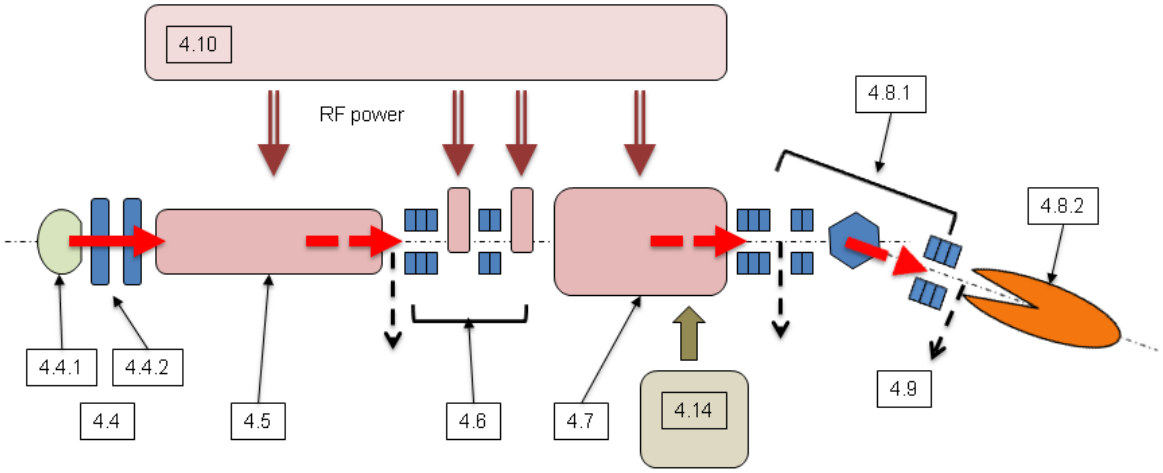

Figure 4. Functional scheme of the LIPAc System.

After control and measurement of the beam parameters, the D^+ current is stopped by a Beam Dump (BD, 4.8.2). Between these systems, specific Medium Energy Beam Transport (MEBT, 4.6) and High Energy Beam Transport (HEBT, 4.8.1) lines transport and match the beam properties to the downstream components.

Amplifier chains (4.10.2), part of the RF Power System (4.10), based on tetrodes, provide the RF power required.

A Cryoplant (4.14) is needed to cool down and maintain the 4.5 K temperature in the SRF Linac. The beam instrumentation (4.9) is distributed along the machine, in addition to the diagnostics included in each subsystem.

The building, completed in Rokkasho in March 2010, consists of an accelerator vault, a nuclear heating, ventilation and air conditioning (HVAC) area, a heat exchange and cooling water area for both radiation controlled and non-controlled areas, an access room, a control room, and a large hall for power racks, RF systems (HVPS and RF power chains) and the 4 K refrigerator (see figure 5). The accelerator vault is surrounded by 1.5 m thick concrete walls and ceiling. The descriptions of the accelerator components, as well as their status, are presented hereafter.

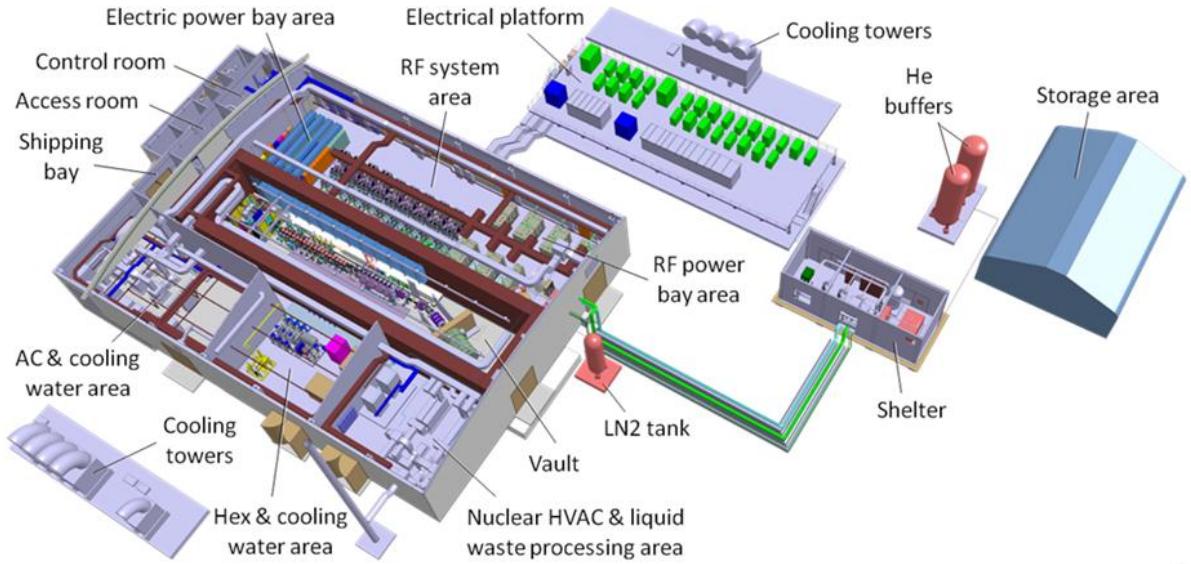

Figure 5. 3D view of the LIPAc facility

IFMIF accelerator, with its 5 MW will become the most powerful Linac in the world, however its prototype, LIPAc will on its own lead the world Linac beam power (see figure 6).

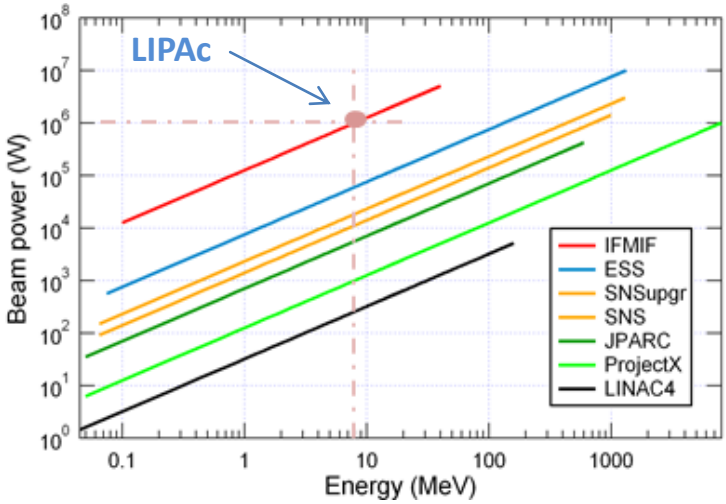

Figure 6. Beam energy vs beam power in existing worldwide hadron Linacs

2.1.1 The Injector + LEBT

The ion source delivers a continuous deuteron beam (140 mA, 100 keV) with high availability and low emittance. It includes an ion source, based on an electron cyclotron resonance cavity, and a Low Energy Beam Transport line (LEBT) to transport and match the extracted beam to the RFQ entrance by means of a dual solenoid focusing scheme (see figure 7 and figure 8) [21, 22]. In addition, an electrostatic chopper will be implemented between the two solenoids to enable the operation of LIPAc with short pulses of very sharp rise/fall times.

The injector was assembled at CEA-Saclay in order to test the components before the arrival in Japan, scheduled at the beginning of 2013. After the first H^+ beam produced in May 2011), a test campaign was carried out in pulsed and continuous operation. Pulsed beams of 150 mA at 100 kV and continuous beams of 100 mA at 75 kV were routinely produced. The first D^+ beam was extracted in April 2012, first in pulsed mode and then in continuous mode for a short period in order to limit the activation of the elements. However, as the continuous operation at 100 kV was limited by HV discharges in the extraction system, a new 5 electrode system (instead of the former 4 electrode system aiming to minimize the beam emittance) has been installed and injector tests started again at the end of September 2012 to complete the optimization (ion source plasma, space charge compensation, solenoid setting) and characterize the beam emittance targeting RMS emittance values lower than 0.25π mm·mrad.

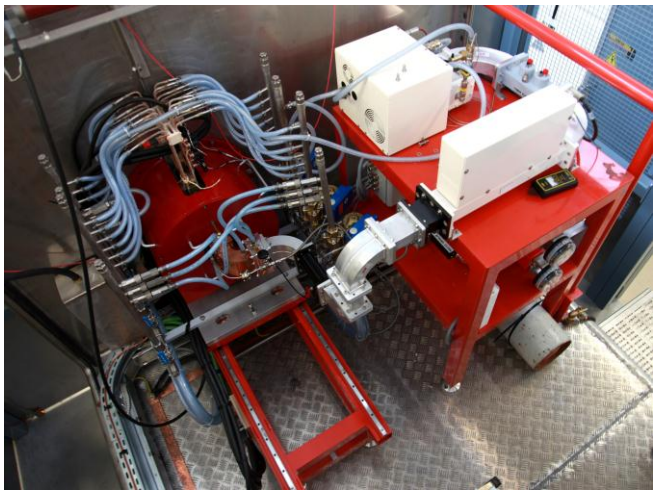

Figure 7. Beam extraction system

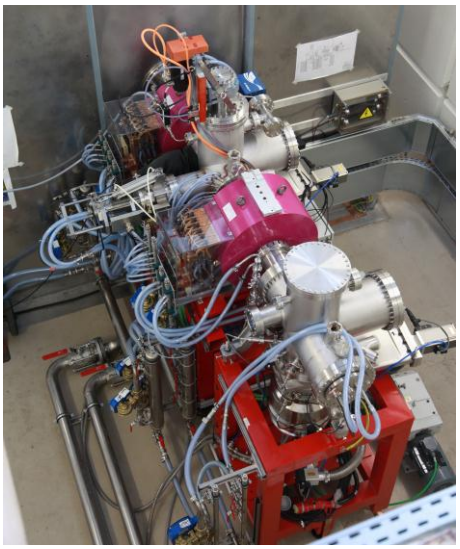

Figure 8. Low Energy Beam Transfer

2.1.2 The Radio Frequency Quadrupole (RFQ)

The 4-vane Radio Frequency Quadrupole (RFQ) under development by INFN, will pre-bunch the DC beam from the ion source and will accelerate the beam from 0.1 to 5 MeV. The 9.8 m long 175 MHz cavity is composed of 18 x 0.54 m long modules flanged together and aligned within 0.3 mm tolerance [23]. The RFQ is the world longest. The peak surface electric field is limited to a maximum value of x1.8 Kilpatrick's criterion [24].

The RF tuning of the RFQ is ensured by 22 slug tuners per quadrant. An aluminium full scale RFQ model was built to validate the tuning procedures and the mode stabilization by means of bead-pull measurements(see figure 9).

After manufacturing, leak tests and dimensional checks of prototype modules to develop the machining and brazing procedures [25], the RFQ module production has started (see figure 10). Three modules (plus the RF plug) have been completed before the end of 2012 for high power tests, planned at the beginning of 2013 at INFN-Legnaro.

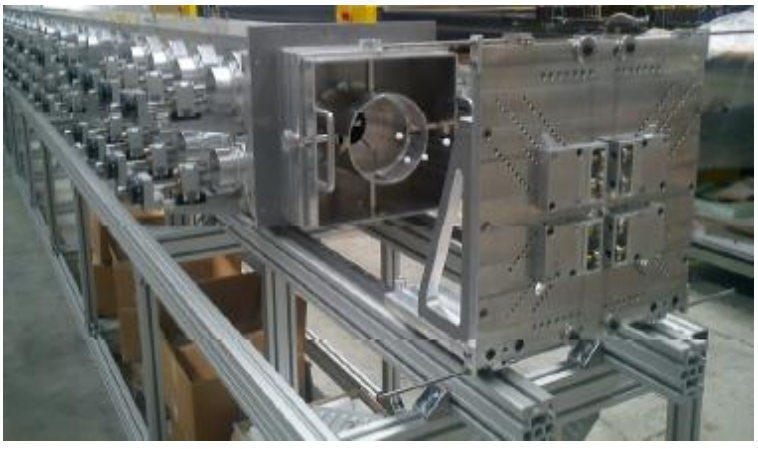

Figure 9. Aluminium full scale RFQ model to validate tuning procedures

The RF power (about 1300 kW) is injected by 8 loop couplers, using 6 1/8" RF windows. High power tests have been performed with a high-Q load circuit at JAEA-Tokai. Final

acceptance tests and RF conditioning in TW mode of two complete couplers (waveguide, window and tip modules) will be performed at INFN-Legnaro on a specific test bench including a coupling cavity. The manufacturing of the other couplers will start just after approval of the acceptance tests [26].

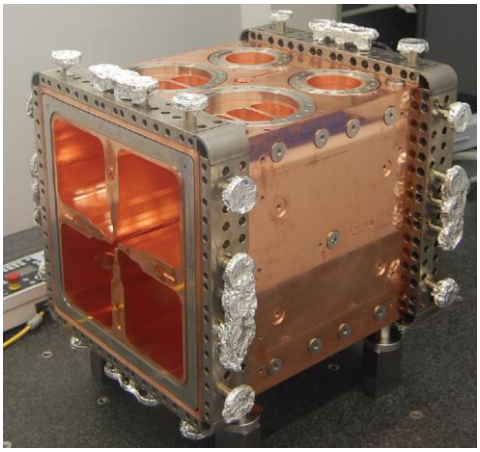

Figure 10. First RFQ module completed (Module 16)

The final acceptance of the entire RFQ will be performed during summer 2014; the final delivery to Rokkasho will take place in October 2014.

2.1.3 The Medium Energy Beam Transport (MEBT)

The main function of the MEBT [27] is to match efficiently the RFQ output beam profile to the SRF input, transversally and longitudinally (see figure 11). The longitudinal forces are applied to the beam by means of two RF resonant cavities. A 5-gap interdigital H-mode configuration has been selected as a buncher cavity as the best compromise in terms of total power dissipation, power density, and space occupied. The radial dimensions of the beam are controlled for injection into the SRF Linac by one quadrupole triplet and one quadrupole doublet. The transverse position of the beam is corrected by the magnetic steerers integrated into the quadrupoles. In order to cut the beam edges and to determine beam losses, the unmatched particles coming from the RFQ are collected by two 4-axis movable metallic plates, called scrapers, inserted between the magnets of the triplet. To achieve the vacuum conditions required by the proximity of the RFQ and Superconducting Radiofrequency Linac, a pumping system in the range of 10^3 l/s for H_2 will be installed at the vacuum ports of the bunchers.

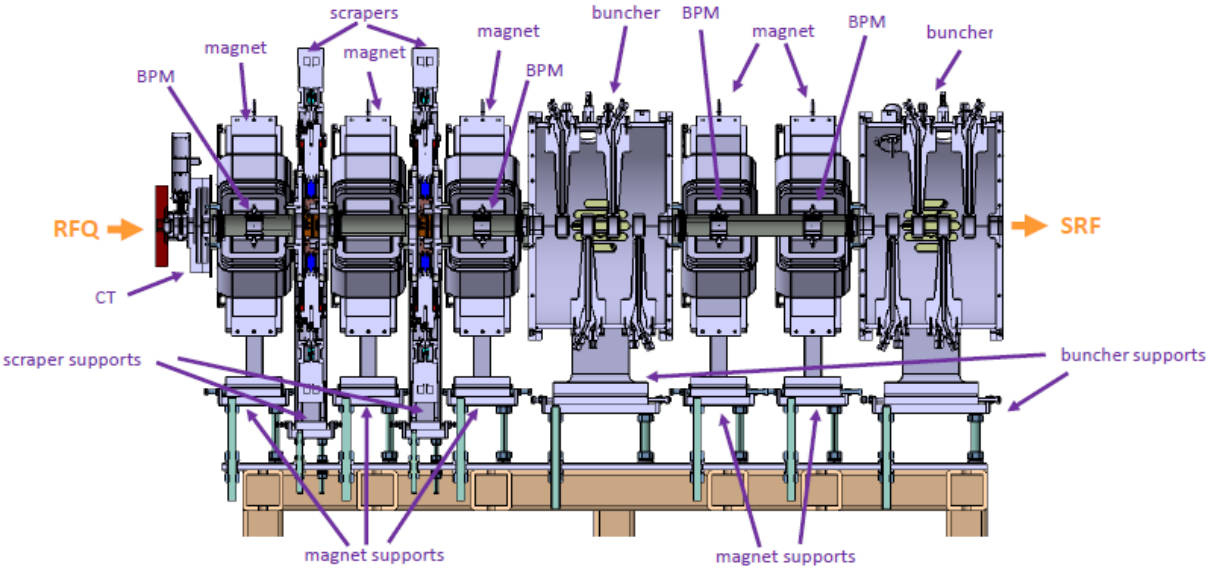

Figure 11. Layout of the MEBT line

The detailed design activities of the main components have been accomplished:

- the magnets have been designed and the first unit was validated on a magnetic test bench in July 2012 ,
- the beam halo and out-of-energy particles coming from the RFQ are stopped in two movable scrapers, designed for a maximum 500 W beam power deposition. It has been designed for easier maintenance and the manufacturing has started for a test which will be done by the end of 2012,
- the bunchers, currently in the detailed design phase, are under study with particular attention to the cooling system, the objective being to comply with the main requirements with an accelerating voltage of 350 kV and a total power of 6.6 kW to be dissipated. A first prototype with aluminum stems for low-power tests is expected before the end of 2012 and the first complete buncher for high-power tests is expected by the beginning of 2013.

In mid-2013 the MEBT will be available for a performance and integration test.

2.1.4 The Superconducting Radio Frequency LINAC (SRF Linac)

The high-energy section of LIPAc accelerates the beam to 9 MeV and consists of the first of the four cryomodules of the IFMIF SRF Linac, housing eight superconducting 175 MHz half-wave resonators (HWR) and eight superconducting solenoid packages [28]. The main cavity and magnet parameters are listed in Table II.

TABLE II: MAIN PARAMETERS OF CAVITY AND SOLENOID

Frequency	175	MHz
Cavity β	0.094	
Accelerating field E_{acc}	4.5	MV/m
Quality factor Q_o	$1.4\ 10^9$	
Max. forward Power / coupler	200	kW
Max. Tuning range	±50	kHz
Beam aperture cavity/solenoid	40/50	Mm
Magnetic field Bz on axis	6	T
Field at cavity flange	≤20	mT

Two prototypical resonant cavities have been fabricated. The original design of the tuner relied on a capacitive plunger with a large membrane to allow an elastic deformation of ±1 mm. Tests at cryogenic temperature showed a low Q_o, as well as a quench at low field, pointing to a suspect NbTi plunger [29]. New tests performed removing the plunger have confirmed the validity of the cavity design (see figure 12).

Figure 12. P02 Half way resonator qualified

As a result, a new design based on a conventional compression tuner principle is under development which leads to a lengthening of the cryomodule to ease the integration of the mechanical tuning mechanism between the HWR tank and the solenoid package.

The RF coupler [30] is composed of a water-cooled Cu antenna, a disk ceramic window, an external conductor made of helium cooled double wall tube and a tee transition between the input coaxial line and the coupler. Two prototype couplers have been fabricated and will be tested on a specific test bench when the 200 kW RF source will be available, planned at the beginning of 2013. The beam focussing and orbit corrections are performed by 8 sets of superconducting solenoids/steerers and beam position monitors, located before each HWR. During the cold tests at 4.2K performed in a vertical cryostat, the theoretical critical current of the magnet was reached (at about 260 A, well above the nominal current of 210 A) with a very short training [31]. The design of the cryomodule, including the magnetic shielding to protect the HWR from the earth magnetic field, two independent 4.5K helium circuits to cool down the cavities and the magnets, a helium phase separator and a thermal shield cooled at 60K by gaseous He, is now almost completed.

2.1.5 The High Energy Beam Transport lines (HEBT) and the Beam Dump

The HEBT line transports the beam from the Linac to the beam dump includes a Diagnostics Plate for beam characterization, a bending magnet to reduce the neutron radiation from beam dump towards upstream components, a magnetic beam expander to limit the power density on the beam dump (< 200 kW/cm^2), a lead shutter, closed during beam shutdown to act as a gamma shield from the activated beam dump and a beam scraper to protect the last portion of the vacuum pipe in front of the beam dump (see figure 13) [32].

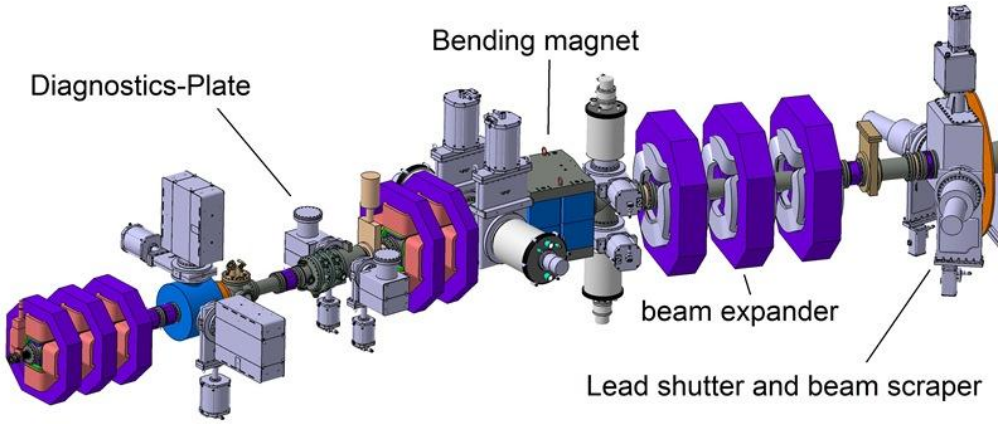

Figure 13. 3D mock-up of the HEBT line

A conical dump [33] made of copper has been designed to stop the 1.125 MW deuteron beam (see figure 14). It is cooled by a high velocity water flow that circulates through an annular channel along the outer surface of the cone. Thermo-mechanical studies showed a high robustness to beam errors, CW and pulsed mode operation, buckling and high velocity coolant flow effects. A local shielding made of water tanks and polyethylene against neutrons and iron blocks against gamma rays associated with an extra frontal shielding made of a 70 cm thick concrete wall to fulfil the radiological protection requirements: low dose rates outside the accelerator vault during accelerator operation and manual maintenance inside the accelerator vault possible during beam-off phases.

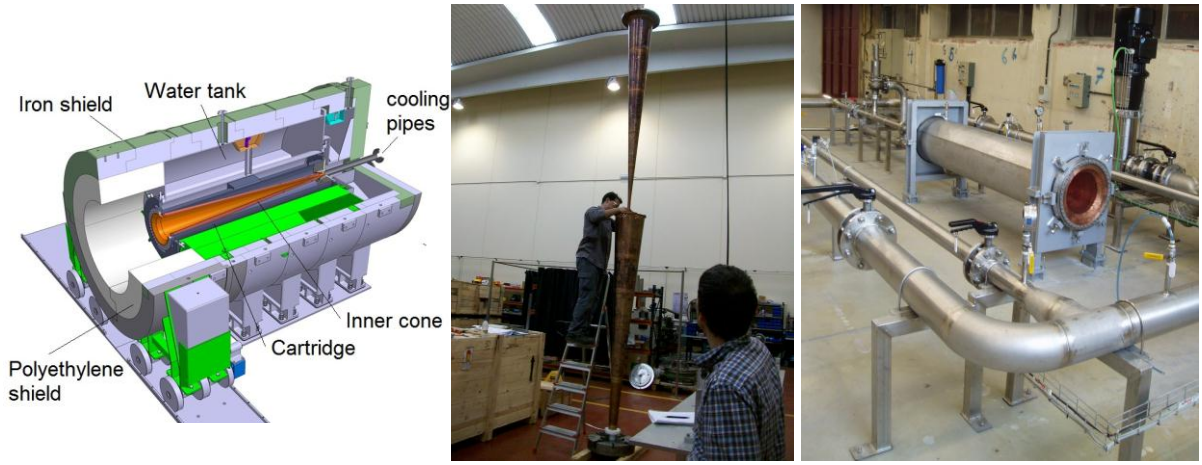

Figure 14. 3D view of the Beam Dump; inner cone installation and cooling tests

The HEBT and the Beam Dump are in the final stage of detailed design, and prototypes of the beam dump cartridge have been built. Hydraulic tests of a 1:1 scale cartridge prototype are on-going. The manufacturing phase will start in autumn 2012 with the integration and test in Europe in mid-2013. The delivery on site will be completed by mid-2014.

2.1.6 Beam instrumentation

Beam instrumentation consists of diagnostics aiming at monitoring and controlling all the necessary beam characteristics along the accelerator (see figure 15), and thus are the basis for its successful operation, right from the early beam commissioning phases up to routine operation. Except for some specific devices, most of the beam diagnostics must therefore be

able to provide information for pulsed and continuous beams equally, withstanding minimum to maximum beam current (power).

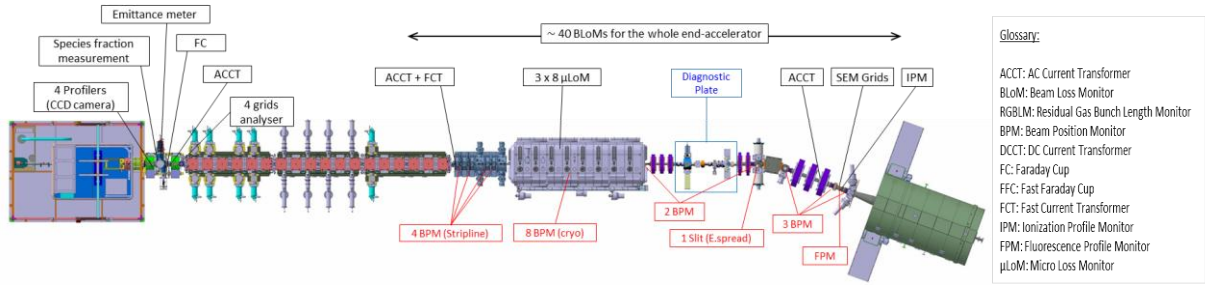

Figure 15. Beam Instrumentation along the LIPAc

A full set of non-intrusive diagnostics to monitor and to characterize the beam all along the accelerator has been developed: current monitors of various types (AC and DC current transformers, fast current transformer), 20 beam position monitors (8 of them at cryogenic temperature), beam profile monitors (based on ionization and fluorescence of the residual gas), around 40 beam loss monitors (ion chamber Large Hadron Collider type), micro-loss monitors (based on chemical vapour deposition) diamond operating at cryogenic temperature), bunch length monitor (residual gas). For short chopped beams, interceptive devices as secondary emission monitor grids and slits will be used for emittance and energy spread measurement [34].
In addition, a Diagnostic plate (D-Plate) combines specific diagnostics to characterize the beam during commissioning with beam, and will be located first at the exit of the RFQ and MEBT during RFQ commissioning, and second at the exit of the SRF Linac during LIPAc normal operation.

2.1.7 RF Power system

The RF Power System [35] is composed of 18 RF power generators to feed the 8 RFQ couplers (200 kW), the 8 superconducting half wave resonators of the SRF Linac (105 kW) and the 2 buncher cavities (16 kW). Except for the buncher cavities, which are fed by full solid-state amplifiers, the same topology has been chosen for all the power chains for standardization and scale economy reasons: they use the same main components (solid-state pre-driver and tetrodes for driver and final amplifier) which can be individually tuned to provide different RF output powers up to 200 kW (see figure 16).

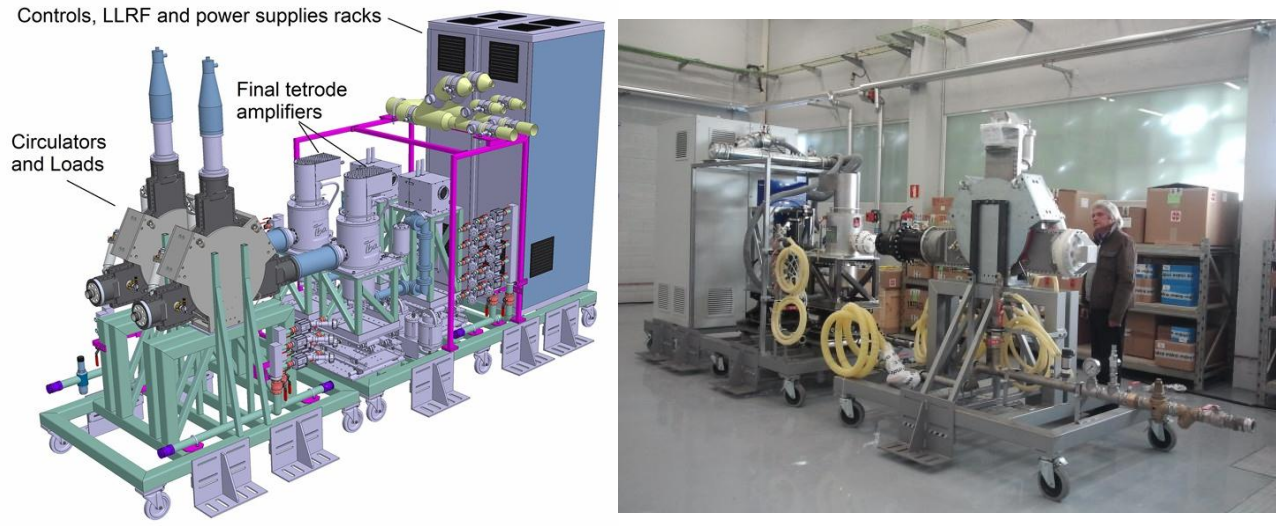

Figure 16. 3D view of the RF Chain 200 kW and 100 kW and Prototype RF module at Madrid Integration facility

The first prototype 200 kW RF source will be ready by the end of 2012 and will be used for the testing and conditioning of the HWR couplers while the first 2 x 100 kW RF module is expected at the beginning of 2013. The 16 kW solid-state amplifier will be ready for the high power tests of the buncher cavities at mid-2013.

2.1.8 Cryoplant

The production of liquid and gaseous helium needed for the SRF Linac cooling is performed with industrial equipment using the well-known Claude refrigeration cycle.
The technical specifications have been completed in 2011 and manufacturing has started in 2013.

2.1.9 Control System

The Control System [36] consists of six subsystems; Central Control System (CCS), Local Area Network (LAN), Personnel Protection System (PPS), Machine Protection System (MPS), Timing System (TS) and Local Control System (LCS).

PPS aims at protecting the personnel against the radiation, the high beam power and other risk factors. In particular, it manages the controlled areas access for radiation safety aspects, while it provides permission/restriction orders for accelerator subsystem actions. After installation of the hardware (PLCs, central console, personnel key box, emergency stops, monitoring cameras) in the building, the programming of the sequence is on going. The Timing System has to include both operation modes (pulsed and cw modes). A TS test bench was developed and was successfully tested on the Injector at CEA-Saclay. MPS controls the beam rapid stop to minimize the beam loss and has to react to an interlock signal in less than 10 μs. The MPS modules have been completed and a test with the interlock circuit of the Injector is planned in November 2012. The MPS logical functions with all subsystems of the accelartor are under progress.

All accelerator subsystems include a LCS connected to the CCS which can work stand-alone under Experimental Physics and Industrial Control System (EPICS) for monitoring and controlling the different subsystem equipment. The LCS development is well advanced for

most of the accelerator subsystems and the development of the Data Acquisition System (DAC), one of the important functions of CCS, is under progress.

All the designs and the definitions of the different structures are under review have been finalized in 2013.

2.1.10 Building, Conventional Facilities and Integration on site

The building, erected in Rokkasho in 2009, consists of an accelerator vault, a nuclear heating, ventilation and air conditioning (HVAC) area, a heat exchange and cooling water area for both radiation-controlled and non-controlled areas, an access room, a control room, and a large hall for power racks, RF systems (HVPS and RF power chains) and the 4K refrigerator (see a photo in figure 17). The accelerator vault is surrounded by 1.5 m thick concrete walls and ceiling.

The installation of the main auxiliaries has been completed, and the remaining components will be provided at the same time as the installation of each sub-system.

All the accelerator system components will be fully or partially tested in Europe before the installation in Rokkasho. To handle the installation on site with all the stakeholders and their respective responsibilities, an integration activity has been set up at the Integrated Project Team level to ensure coherence, and that all the requirements are fulfilled.

Figure 17. Accelerator building in Rokkasho

To ease this process different tools have been implemented such as a Plant Integration Document (LIPAc PID), a baseline document of the project, an Interface Management System (IMS), defining and detailing all the interfaces between each sub-system, and a 3-dimensional integration review process to insure the coherency of the integration on site.

2.2 Lithium Target Facility Validation Activities

The EVEDA tasks related to the Li target facility validation consist of 4 activities which cover the construction and operation of a Li test loop including purification systems, diagnostics for the Li target, erosion/corrosion tests of loop structure materials and remote

handling aspects of the target assembly. The activities are jointly carried out by JAEA and ENEA.

2.2.1 ELTL flow validation and purification systems

The EVEDA Lithium Test Loop (ELTL), physically almost equivalent to the loop in the IFMIF Plant [12], has been built at Oarai and successfully commissioned in February 2011 with an "integral concept" target assembly manufactured in stainless steel (figure 18). The design was carried out from March to December 2009 and the construction was completed by November 2010. The loop consists of three floors with a total height of approximately 20 m from the ground level and a pit in which the dump tank is placed. A simplified piping and instrumentations diagram (P&ID) is shown in figure 19. The ELTL is composed of two major branches which are the main loop with 6"/8" piping and the purification control loop with a 1" piping. All piping is made of AISI 304 steel. The main loop contains the target assembly, a quench tank, an electro-magnetic pump (EMP), an electro-magnetic flow meter (EMF), a Li cooler and the dump tank. The tanks connect to Ar gas cylinders and turbo-molecular vacuum pump units to control pressure and vacuum.

Figure 18. ELTL just commissioned in the JAEA premises in Oarai

The ELTL is able to generate a flow rate of 3000 l/min which will produces a flow velocity of 20 m/s in the target assembly. It can operate at Ar pressure and in a vacuum condition of 10^{-3} Pa [13].

The target assembly is installed at the 3rd floor inside of an air-tight vessel, which is filled with Ar during operation. The target assembly is equipped with a double reducer nozzle and a concavely curved open channel of 100 mm width (2.6 times reduced compared to IFMIF) to generate a free surface Li jet of nominal 25 mm thickness like in IFMIF [37].

A Li flow at IFMIF nominal velocity of 15 m/s was achieved in the target assembly with an Ar gas pressure of 0.12 MPa. In September 2012, the loop was back in operation after the damage suffered at the time of Great East Japan earthquake. During this restoration work, the first test operation was conducted to gain critical information about the geometrical stability of the lithium flow and the performance of the flow guiding structure up to 20 m/s flow speed.

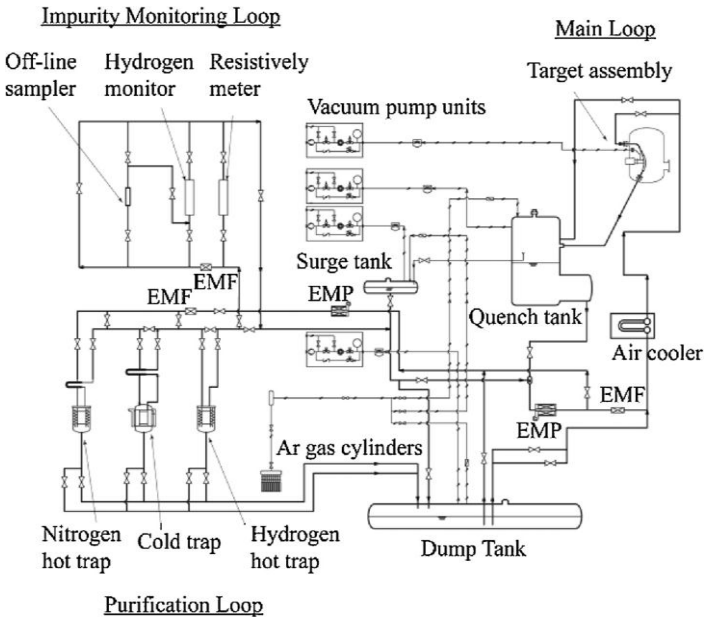

Figure 19. Layout of the ELTL (some traps and monitors are not yet installed)

The purification loop is connected to the main loop at the upstream and downstream of the EMP. An impurity monitoring loop is branched at the downstream of the impurity traps in the purification loop. The purification loop includes a cold trap that removes oxygen, and two mechanical interfaces to install two hot traps to remove nitrogen and hydrogen respectively. These two hot traps are designed and fabricated in collaboration with Japanese universities, who qualify the getters in a separate task. These traps will be installed in the future. The N content is considered particularly critical, since it has a strong impact on corrosion and erosion through the formation of Li ternary nitrides Li_3CrN_2. The trap must therefore reduce the N content to values < 10 ppm, but the methodology followed; i.e. a getter made of pellets of Fe doped with Ti, has currently still shown limitations.

The impurity monitoring loop includes a Li sampler to analyze impurity concentration in the Li off-line, and interfaces to two on-line monitors, which will be installed in the future.

The dump tank is capable to store the 2.5 tons of Li that were melted from 1608 ingots. The installation was particularly laborious in a purposed design glass-box to limit the contamination by air and humidity (values below 25 ppm was ensured). Figure 20 shows the interior of the glove box with some Li ingots sealed in plastic.

Figure 20. Glove box with Li ingots

2.2.2 Target diagnostics

The diagnostics for the free surface cross-flowing Li jet in the target assembly exposed to vacuum that will absorb the 10 MW beam power is of utmost relevance. The thickness and the waviness of the jet must be controlled to ensure sufficient Li screen to absorb the beam energy, which presents its peak for deuterons at 40 MeV at 19 mm. A contact probe has been developed with a minute needle that does not generate visible turbulences that drops voltage at contact with flowing Li. It has been successfully applied to measure jet thickness and wave heights at the Li loop of the University of Osaka (figure 21) [37]. Its adaptation to the ELTL is still to be proven and to the high radiation environment of IFMIF is still to be done.

A new optical method by means of time-of-flight of a laser beam has been developed and tested by Osaka University with a precision of 1 μm. Applicability at the ELTL has been proven in preliminary tests.

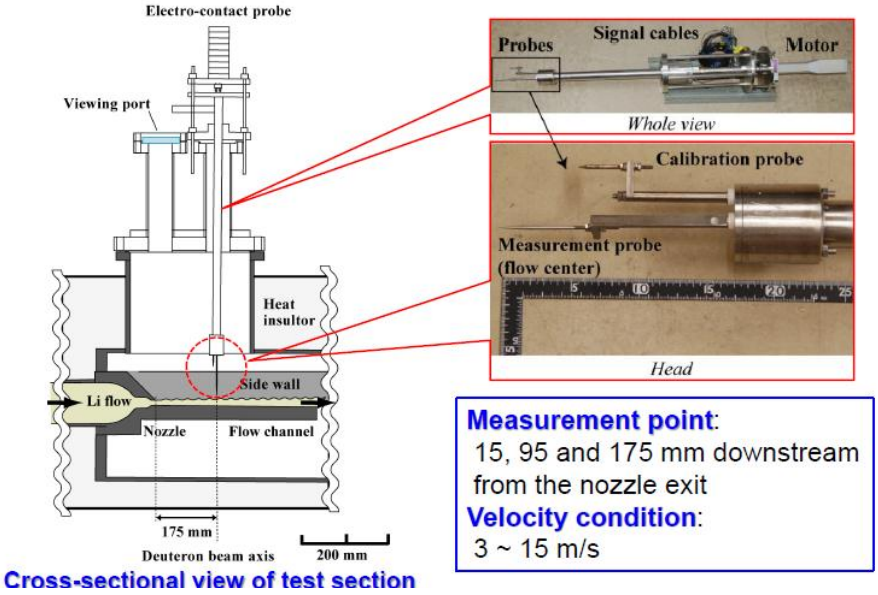

Figure 21. Set up of the contact probe measurement in the Osaka Li loop

A thorough analytical assessment of the wave height distribution combined with CFD modelling has managed to predict the pattern with Görtler vortices under Rayleigh-Taylor instabilities. Wave amplitudes are inversely proportional to liquid Li speed and with 90% of probability the nozzle will guarantee surface amplitudes within the 1 mm specified. Speed influence in wave pattern can be observed in figure 22 from Osaka Li loop.

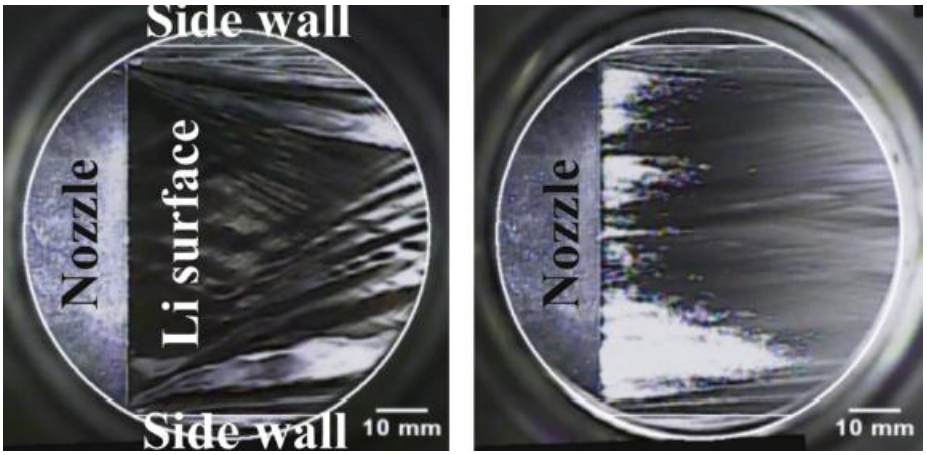

Figure 22. Flow pattern close to the nozzle at two velocities (Osaka Li loop). Amplitude is observed as to be inversely proportional to Li liquid speed

2.2.3 Erosion/corrosion testing in LIFUS6

Dedicated corrosion/erosion tests for austenitic and RAFM steels were planned with the existing LIFUS3 loop at ENEA-Brasimone but certain limitations to accomplish the expected validation activities led to the construction of a new liquid Lithium test facility in 2010. The new loop LIFUS6 (see plant layout in figure 23) is built with a simplified configuration from the hydraulic point of view and contains a cold trap operated continuously in a bypass stream and a hot (nitrogen) trap based on Ti-sponge operated in batch [14]. The Li will flow under isothermal conditions at 350°C. The maximum velocity in the test section will be about 16

m/s. The impurities will be measured on-line by a resistivity meter developed by ENEA and University of Nottingham; it relies on the linear variation of the metal resistivity at a given T with the concentration of N anions, and by the chemical analysis of Li samples. A resistivity meter will be sent to Oarai to be integrated in the ELTL.
The experimental program foresees up to 8000 hours of corrosion/erosion tests, which will start in spring 2013.

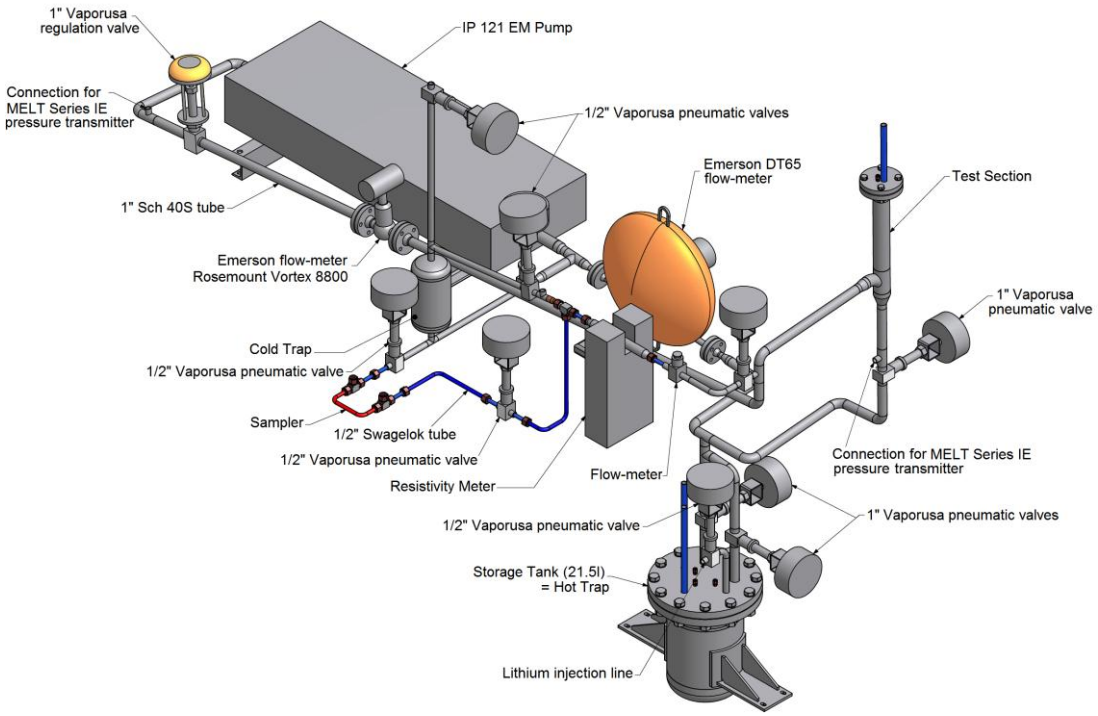

Figure 23. Layout of the LIFUS6 loop in Brasimone (ENEA)

2.2.4 Remote handling validation

A dedicated orbital Laser welding machine has been developed by JAEA to remotely weld and cut a lipseal flange. The process has been validated using a mock-up of the IFMIF inlet pipe in collaboration with Osaka University. Figure 24 shows a welding trial. The flanges are made of AISI 316L steel and the peripheral lips are 2+2 mm thick. A 16 kW fibre laser is used. Welding and cutting is done with a power of 5 kW beam power and a speed is 3m/min. Welding quality is acceptable, but cutting still needs to be improved to avoid sticking of the flanges and proper weld geometry for re-welding the same lips. In addition, quality procedures to be applied remotely need to be developed.

At ENEA, a target assembly mockup is under construction to simulate remote replacement of a removable backplate based on the bayonet concept and detachment and reconnection of flanges fastened with a dedicated connection system developed at the institute. The tests will simulate the geometrical constraints of the test cell using a manipulator system similar to that planned for IFMIF.

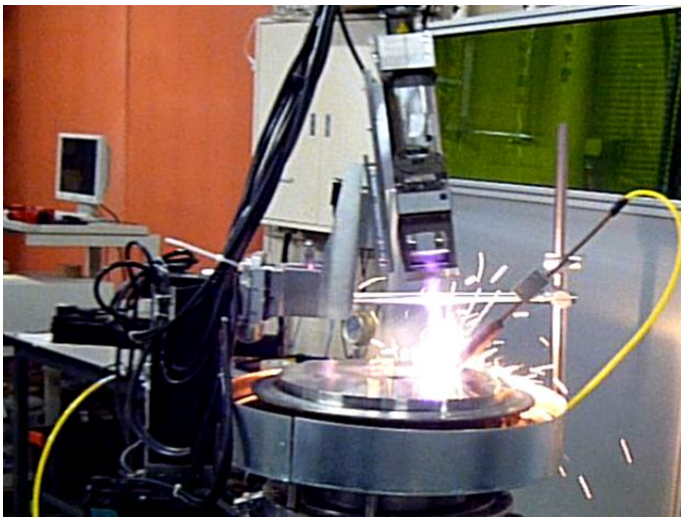

Figure 24. Weld trial with the orbital fiber laser system in Osaka University

2.3 Test Facility Validation Activities

The design and validation of the test facilities are predominantly conducted in the European Home Team with the exception of the Small Specimens Test technique development carried out under the coordination of Japanese Home Team. Design work of the test facilities is accompanied by prototyping of the High Flux Test Module (HFTM) and internal rigs for post-irradiation examination of miniature-size specimens of fusion reactor materials and on-line creep testing in the Medium Flux Test Module (CFTM). It is also making progress on the design and R&D of an alternative proposal of HFTM, potentially enabling irradiation under very high temperatures, adequate for irradiation testing of SiC [16].

2.3.1 High Flux Test module

The irradiation of small specimens is planned at several blanket-relevant irradiation temperatures and shall accumulate structural damage of up to 150 NRT dpa. The HFTM will allow the irradiation and the temperature control of the specimens by an active cooling system of He gas. The HFTM is mainly dedicated to the research on RAFM steels, to be tested in the temperature range 250-550°C, with an option to provide irradiation up to 650°C. The uncertainty of temperature for 80% of the specimen is demanded to be below +/-3% related to the absolute nominal temperature. Further, it is an aim to cool the specimen from their temperature to below 200°C to freeze the irradiation defects after the irradiation within 15 minutes. The arrangement of the specimens in the HFTM is adapted to the beam footprint of the neutron source, which is 20 cm x 5 cm. The specimen alignment, and the dimensioning of reflectors, must limit the neutron flux gradient to less than 10% of the individual sample gage volume. In order to transmit the neutron flux with as little as possible losses to the specimens, the HFTM structures need to be thin, and avoid materials with a high neutron absorption cross section. A minimum of 26, but possibly up to 40 specimens per alloy, should be accommodated for a single irradiation position. The structures of the HFTM might be exposed to damage rates of up to 50-55dpa/fpy but are submitted to stresses [15].

The HFTM is built from a thin walled container divided into eight compartments, into which three rigs can be placed in each (for a total of 24 rigs). The central four compartments (360 cm^3 for specimens) are inside the beam footprint where neutron flux levels are suitable for

high quality irradiation experiments. The remaining four out-of-center compartments are also filled with rigs. The function of these so called companion rigs is mainly to act as lateral neutron reflectors, but also to accommodate instrumentation, like fission chambers for online flux monitoring. In the two compartments located at the lateral ends most distant from the source, the neutron flux amounts to only about 10% of the central positions, but flux gradients are low, and can thus be attractive as additional irradiation space.

The specimens are contained in rectangular irradiation capsules (external dimensions 120 mm x 46.7 mm x 13.4 mm) equipped with electrical heaters, which can partly compensate the spatial distribution as well as temporal fluctuations of the nuclear heat release. In order to homogenize the temperature field, gaps between the specimens are to be filled up with liquid NaK-78 eutectic alloy (see figure 25). The capsules are encased inside irradiation rigs, which incorporate neutron reflectors on the upper and the lower end. In order to guarantee the severe temperature gradient allowed, gaps between encapsuled specimens are filled up with liquid NaK-78 eutectic alloy. The capsules are encased inside irradiation rigs, which incorporate neutron reflectors on the upper and the lower end. A helium gas flows between the capsule surface and the rig functions as the main thermal resistance between the specimen and the heat sink with a maximum gap of 1.35mm depending of the capsule target temperature level (250-650°C). In turn, the irradiation temperature is measured and controlled thanks to various (between 3 and 6) type-K thermocouples located inside the specimen stack. The thermocouple readings will be the input to the control of the capsule's electric heaters. In the current design, the thermocouples are directly immersed in the NaK of the specimen stack.

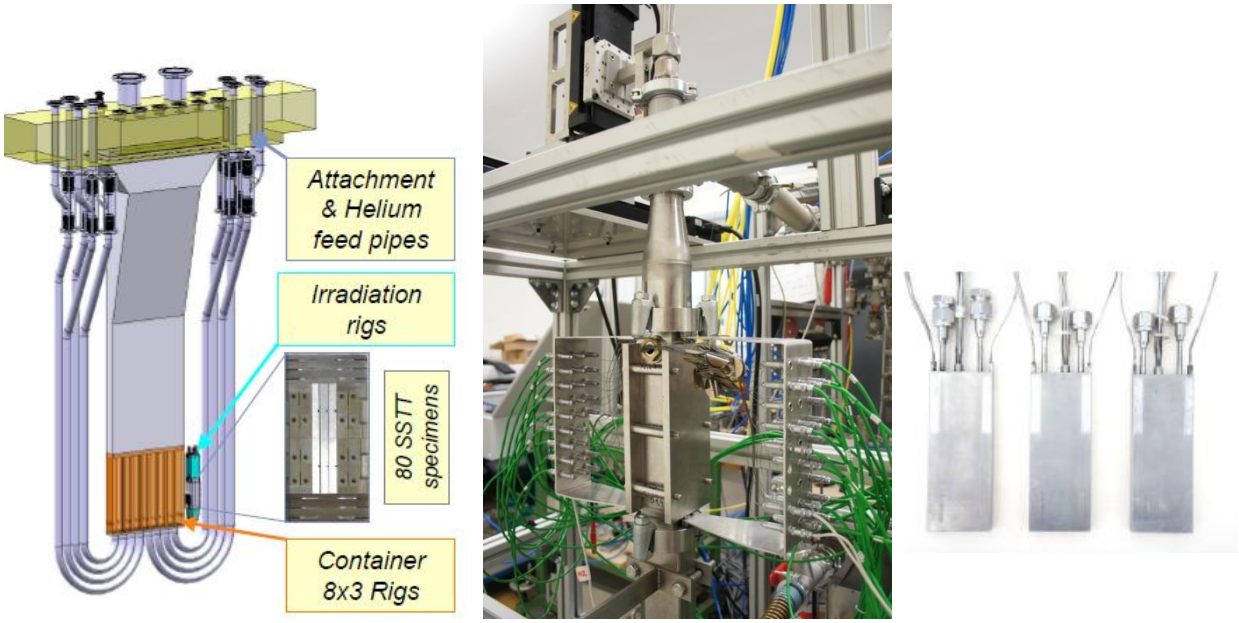

Figure 25. HFTM 3D model and final constructed under tests. On the right, capsules filled with NaK

The capsules will be tested under irradiation conditions realized in the Belgian BR2 research reactor [17]. This irradiation will provide nuclear heating of approximately 3W/g as in the HFTM, but obviously considerably lower total doses than anticipated for IFMIF end-of-life can be accumulated in this campaign. Main objectives are the test of the heaters and the capsule temperature control, but also the recovery of the specimens after irradiation under

hot cell conditions. Such experience will be most valuable for the planning of the IFMIF hot cells and related logistics and workflow optimization.

The last step of validation will be the testing of a 1:1 prototype HFTM will be installed in the HELOKA-LP helium loop facility at KIT (see figure 26), where it will be operated under IFMIF design operation conditions, in what regards mass flow (up to 120 g/s), gas pressure (0.3 MPa) gas temperature and electrical heating of the capsules [18]. The test objectives include the verification of the temperature control strategy, assessment of flow induced dynamic loads on the rigs, the attachment structure and the helium pipes, and the definition of operational modes (startup/shutdown, emergency stops, cooldown transients etc.)

Figure 26. HELOKA-Li loop facility at KIT (Karlsruhe)

2.3.2 Medium Flux Test Module or Creep Fatigue Test Module

The purpose of the Creep Fatigue Test Module (CFTM) in IFMIF is to perform creep fatigue experiments under intense neutron irradiation [19]. The CFTM consists of three parallel testing machines, mounted on a frame, which is operated independently. It will be installed in the medium flux area of the test cell and will be exposed to intense radiation fields, including both neutron and gamma fields. The heat absorbed by the different parts of the module will be extracted by means of a He gas passing through independent cooling channels. Measures to learn the temperature and control it in the specimen under testing to ensure that the target values are respected will be also included.

The testing machine load cells and extensometers have been designed to withstand the hard operation conditions of irradiation and temperature.

The final CFTM will consist of three parallel load controlled single testing machines (STM), mounted on a frame. The three testing machines will operate independently with +/-12.5 kN load with controlled speed ranging between 1 μm/s and 80 μm/s (see figure 27). The results obtained for a STM are conferrable to the second and third STMs. Finally, the complete CFTM will be installed in the medium flux area of IFMIF test cell and will be exposed to intense radiation fields, including both neutron and gamma fields. The heat absorbed by the different parts of the module will be extracted by means of a helium gas (coolant) passing through independent cooling channels. Elements required to control the specimen temperature at the targeted value will be included. The first tests have been performed without radiation and heating effects.

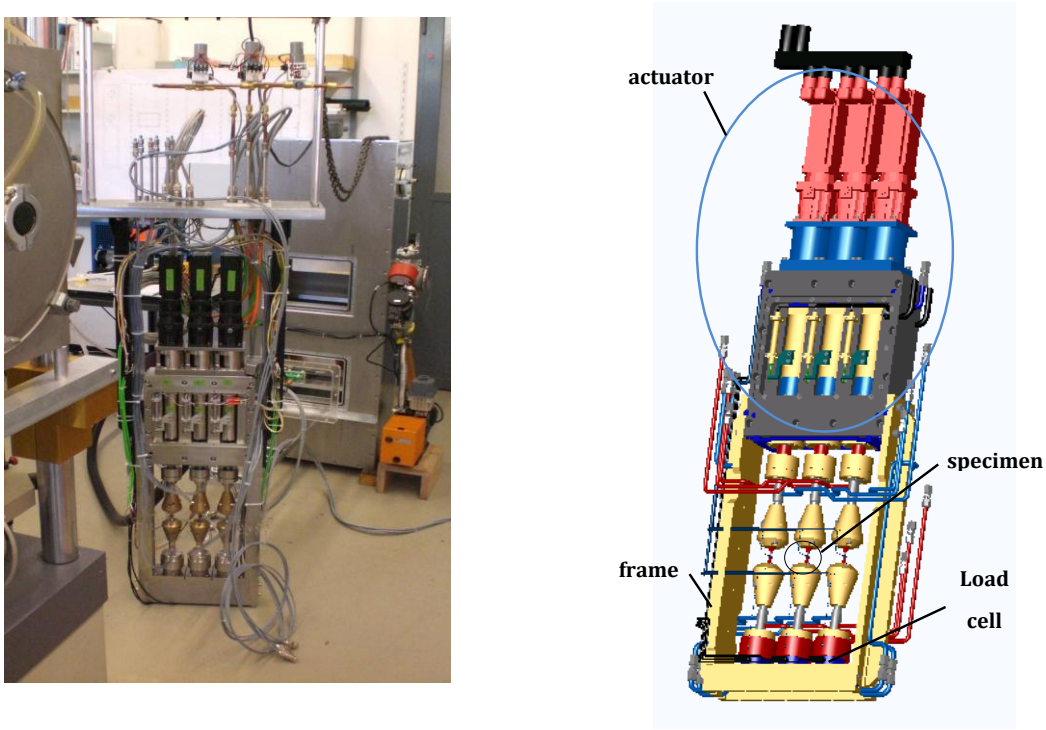

Figure 27. CFTM 3D model and final constructed equipment

2.3.3 Small Specimen Test Technique

Due to the limited irradiation volume available in the test modules, small specimen test technique (SSTT) is being developed under IFMIF/EVEDA frame by various Japanese universities (College of Hachinohe, Kyoto University and Tohoku University) and institutions (NIFS) under the coordination of JAEA [38]. The understanding fracture mechanics of irradiated specimens as well as fatigue behavior in the irradiated materials of the first wall in the fusion reactor vessel is essential.

Tests have been carried out with specimens fabricated with the RAFM F82H. The reduction in size from standard size specimens has been demonstrated achievable for some types.

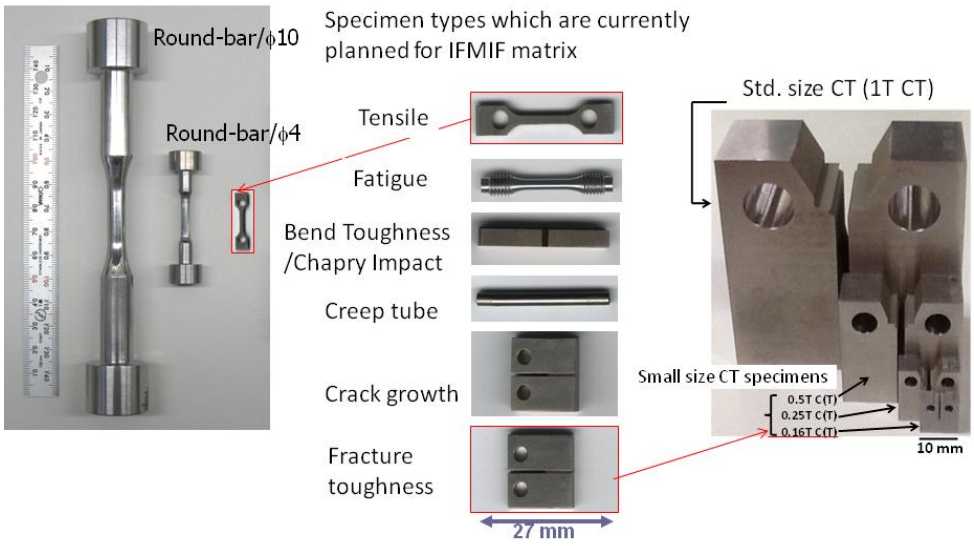

Figure 28. Small specimens devised for fusion materials testing

Two types of fatigue specimens were tested with a perfect match for the round bar type in the range of interest as shown in figure 29. Further tests are needed to understand a slight deviation from the expected hysteresis behaviour.

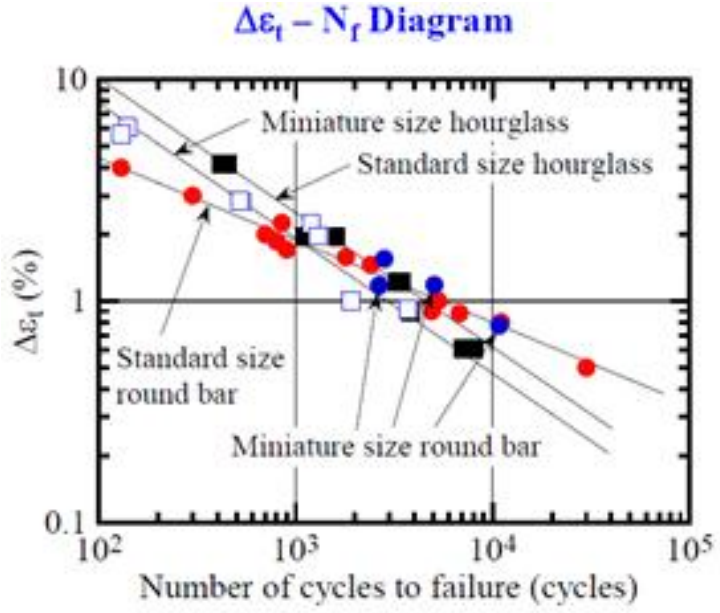

Figure 29. Fatigue testing comparison of standard specimen with two types of small specimens

Transition fracture toughness has been measured with ¼CT-specimens aiming at the definition of Master Curve (MC) following ASTM E1921 'Determination of Reference Temperature, To, for Ferritic Steels in the Transition Range'. Results indicate that the correlation developed for ferritic steels cannot be exactly applied (see figure 30). A new correlation has been proposed, but further tests are needed to statistically secure it. The impact of cold work on toughness to simulate irradiation effects has been investigated for F82H. Whereas standard Charpy specimens correlate well, it has been shown that CT-specimens do not follow that trend and it cannot replace the impact of irradiation at the spectrum and flux to be expected in a fusion power plant. It is to be noted that Charpy tests for minituarized specimens is already covered by ASTM E1253 'Reconstitution of Irradiated Charpy-Sized Specimens'.

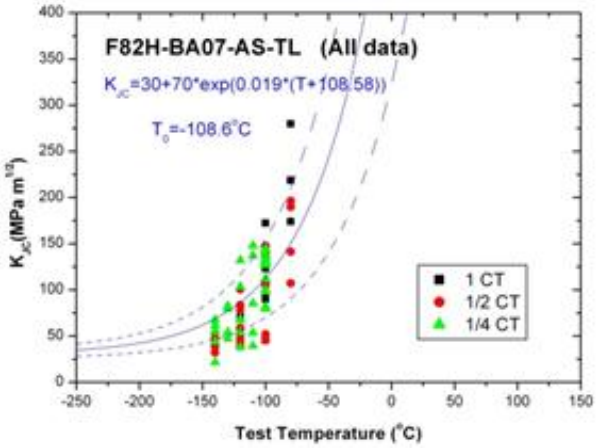

Figure 30. Fracture toughness measured following ASTM 1921 fitting with the Master Curve for standard specimens

The crack growth rate through environmental assisted cracking and stress corrosion cracking, well known effects in austenitic steels for fission reactors, has been assessed for RAFM by Hachinohe College with no significant difference observed with the data accumulated with austenitic steels.

2.3.4 Fission chamber

Fission chambers (FC) will give information (on-line) on the Test Cell irradiation conditions. Although these detectors are commonly used in power plants, the detector functioning in the harsh environment of the Test Cell must be proved. Therefore, validation experiments had to be performed under conditions as close as possible to the IFMIF ones.

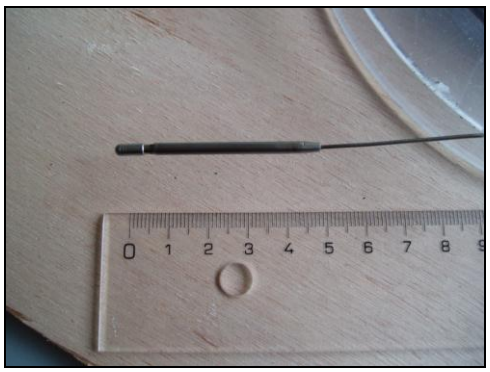

Figure 31. Prototype of the fission chamber, model CFUR43/C5B-U8.

During 2008 two prototypes (one FC and one ionization chamber) were acquired. For studying the FC behavior in an environment free of neutrons, they were tested in an X-rays and in a ^{60}Co irradiation facilities at CIEMAT. After these preliminary tests the detectors were sent to the BR2 reactor (SCK·CEN) for monitoring fast neutron fluxes. The integrated gamma absorbed dose was about $4x10^{10}$ Gy and the fast neutron fluence (E > 0.1 MeV) $4x10^{20}$ n/cm^2. Figure 32 shows the comparison between calculated values and experimental data in three BR2 different channels [39]. Fission rates were calculated with ACAB code, while the final FC current was calculated through a numerical code developed at CIEMAT.

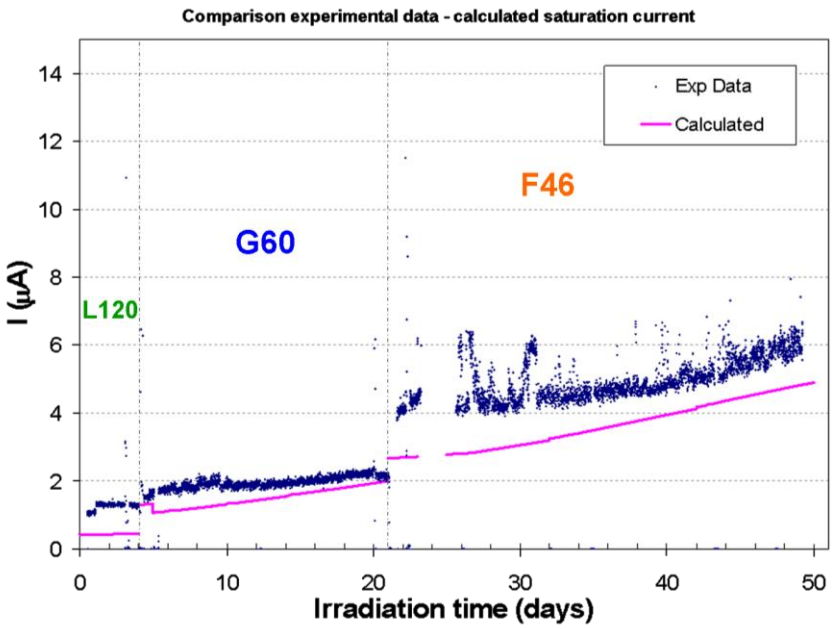

Figure 32. Purely neutron-induced signal of the FC after gamma subtraction (points) and comparison with theoretical calculation (solid line). The numbers above the data indicate different BR2 irradiation channels, from ref [39].

New prototypes have been acquired and will be included in the new BR2 irradiation [17], with the main objective of demonstrating the detectors robustness under an intense neutron flux. Validation of theoretical calculations will be also possible.

3. Conclusions

The world fusion programme needs neutron sources adapted to its own physical requirements. ITER and NIF will teach us how to control deuterium-tritium nuclear fusion reactions under electromagnetic and inertial confinement, however the mechanical properties that essential building bricks will show after few years of operation of a fusion power plant remain unknown. Licensing of a fusion reactor will not be possible without an understanding of the degradation during operation of the materials of its vessel directly exposed to the nuclear reactions. The successful development of nuclear fission power plants in the 50s demanded a parallel intense materials research over decades to understand the impact of fission neutrons in structural materials [40]. Present maturity of materials science and modern computation techniques can guarantee a thorough understanding of the behaviour once relevant data is available; unfortunately the spectrum and flux of either existing or planned fission or spallation neutron sources cannot disclose the unknowns. The transmutation energy threshold for p^+ and α-particles generation goes beyond typical fission neutrons energy including fast breeder reactors; in turn, spallation sources present wide neutron spectra with long tails reaching one order of magnitude higher energy than fusion neutrons (with the generation of typically one order of magnitude more appm/dpa of He leading to a significantly more severe embrittlement). Furthermore, direct extrapolation of the mechanical degradation under irradiation from a FCC crystal structure of austenitic steels to the ferritic BCC is not possible. Fusion relevant data at 30 dpa is needed to meet nuclear fusion roadmaps [41]. IFMIF will generate neutrons with a broad peak at 14 MeV at a flux of 10^{18} /m·s^2 that will allow materials testing at equivalent conditions of those in a fusion power plant. The impact of temperature while irradiation takes place in the detrimental lattice void swelling (observed for ferritic-martensitic steels from 20 NRT dpa) is known; the High Flux Test Module (under validation in Karlsruhe) present 24 independently cooled capsules that will allow the tuning of the optimal operational conditions of a power plant. Furthermore, the small specimens technique is mature; it will provide an understanding of macroscopical properties. Its standardization would be of global benefit. The fusion materials programme demands joining forces, unravelling the physics through suitable testing will validate and tune existing neutronics models and will allow the design of radiation harder low activating materials, with an enormous impact on fusion power plant operational life. Moving towards electricity production demands materials science, in parallel with alternative facilities targeting to tame nuclear fusion reactions, to play a key role in the world fusion programme endeavours. Suited material testing experimental facilities are indispensable; IFMIF is.

Acknowledgement

The authors wished to thank all the members of the Integrated Project Team (Project Team in Rokkasho, JA Home Team in Tokai and Rokkasho and the EU Home Team at Garching) and at the various Research Centers of the European Countries being Voluntary Contributors to IFMIF/EVEDA and Japanese Universities and research centers.

This paper has been prepared within the framework of the BA Agreement between Japan and EURATOM.

The views and opinions expressed herein do not necessarily reflect those of CIEMAT, ENEA, F4E, JAEA or KIT.

References

[1] Norgett, M.I. et al, “A proposed method of calculating displacement dose rates”, Nucl. Eng. Des. 33 (1975) 50-54

[2] Ehrlich, K., Bloom, E., Kondo, T., “International strategy for fusion materials development”, J. Nucl. Mater. **283–7** (2000) 79

[3] IFMIF International Team, “IFMIF Comprehensive Design Report”, IEA on-line publication,http://www.iea.org/Textbase/techno/technologies/fusion/IFMIF-CDR_partA.pdf and partB

[4] Gilbert, M.R. “An integrated model for materials in a fusion power plant: transmutation, gas production, and helium embrittlement under neutron irradiation”, Nucl. Fusion 52 (2012)

[5] Vladimirov, P., Moeslang, A., “Comparison of material irradiation conditions for fusion, spallation, stripping, and fission neutron sources”, J. Nucl. Mater. **329-33** (2004) 233

[6] Nishitani, T., et al., “Progress of fusion nuclear technologies in the broader approach frame work”, Fusion Eng. Des. **87** (2012) 535

[7] Heidinger, R., Sugimoto, M., “Progress in IFMIF Engineering Validation and Engineering Design Activities (IFMIF/EVEDA)”, Proceedings of SOFT2012, Liege

[8] Garin, P., “Start of the engineering validation and design phase of IFMIF”, J. Nucl. Mater. **386-8** (2009) 944

[9] Moeslang, A. IFMIF: the intense neutron source to qualify materials for fusion reactors, C.R. Physique 9 (2008) 457-468

[10] Mosnier, A., “Status of the IFMIF/EVEDA 9 MeV 125 mA deuteron linac”, Proceedings of LINAC2012,Tel Aviv

[11] Cara, P., et al., “Overview and status of the Linear IFMIF Prototype Accelerator (LIPAc), Proceedings of IAEA Fusion Energy Conference 2012, San Diego

[12] Molla, J., Nakamura, K., “Overview of the main challenges for the engineering design of the test facilities system of IFMIF”, Fus.Eng.Des. **84** (2009) 247

[13] Kondo, H., et al., “Completion of IFMIF/EVEDA lithium test loop construction”, Fus. Eng. Des. **87** (2012) 418.

[14] Aiello, A., et al., “Lifus (Lithium for Fusion) 6 loop design and construction”, Proceedings of SOFT 2012, Liege

[15] Arbeiter, A., et al., “Overview of results of the first phase of validation activities for the IFMIF High Flux Test Module”, Fus. Eng. Des. **87** (2012) 1506.

[16] Abe, T., et al., “SiC/SiC composite heater for IFMIF”, Proceedings of SOFT 2012, Liege

[17] Gouat, P., et al., “Present status of the Belgian contribution to the validation and design activities for the development of the IFMIF radiation-testing modules”, Fus. Eng. Des. **86** (2011) 627.

[18] Schlindwein, G., et al., “Start-up phase of the HELOKA-LP low pressure helium test facility for IFMIF irradiation modules”, Fus. Eng. Des. **87** (2012) 737.

[19] Vladimirov, P., et al., “Nuclear responses in IFMIF creep-fatigue testing machine”, Fus. Eng. Des. **83** (2008) 1548.

[20] Gex, D., et al., “Engineering progress of the Linear IFMIF Prototype Accelerator (LIPAc)”, Proceedings of SOFT 2012, Liege

[21] Gobin, R. et al., “General design of the International Fusion Materials Irradiation Facility deuteron injector: Source and beam line”, Rev. Sci. Inst. 81, 02B301 2010

[22] Gobin, R., “Light ion ECR sources state of the art for Linacs”, Proceedings of LINAC2012, Tel Aviv

[23] Pisent A., et al., “Production and testing of the first modules of the IFMIF-EVEDA RFQ”, Proceedings of IPAC12, New Orleans

[24] Kilpatrick, W.D., Criterion for Vacuum Sparking Designed to Include Both RF and DC, Rev. Sci. Instrum. 28, 824 (1957)

[25] Pepato, A. et al., “Mechanical Design of the IFMIF/EVEDA RFQ”, Proceedings of PAC09, Vancouver

[26] Maebara, S., “Coupling cavity design of RF input coupler tests for the IFMIF/EVEDA RFQ”, Proceedings of IPAC12, New Orleans

[27] Podadera, I., “The Medium Energy Beam Transport Line (MEBT) of IFMIF/EVEDA LIPAc”, Proceedings of IPAC11, San Sebastián

[28] Orsini, F. et al., “Preliminary Results of the IFMIF Cavity Prototypes Tests in Vertical Cryostat and Cryomodule Development”, Proceedings of the Superconducting Radio Frequency Conference’11, Chicago

[29] Bazin, N., “Thermo-Mechanical Simulations of the Frequency Tuning Plunger for the IFMIF Half-Wave Resonator”, Proceedings of LINAC2012, Tel Aviv

[30] Jenhani, H., “Input power coupler for the IFMIF SRF Linac”, Proceedings of IPAC12, New Orleans

[31] Sanz, S., “Fabrication and Testing of the First Magnet Package Prototype for the SRF Linac of LIPAc”, Proceedings of IPAC11, San Sebastián

[32] B. Brañas et al., Design of a beam dump for the IFMIF-EVEDA accelerator, Fusion Engineering and Design 2-6 (2009) 84

[33] Iglesias, D., et al., “The IFMIF/EVEDA Accelerator Beam Dump Design”, J. Nucl. Mater. **417** (2011) 1275

[34] Marroncle, J., “The IFMIF/EVEDA LIPAc Diagnostics and its Challenges”, Proceedings of IBIC 2012, Tsukuba

[35] Regidor, D., “IFMIF-EVEDA RF Power System”, Proceedings of IPAC11, San Sebastián

[36] Takahashi, H., “Development Status of PPS, MPS and TS for IFMIF/EVEDA Prototype Accelerator”, Proceedings of IPAC11, San Sebastián

[37] Kanemura. T. et al., Investigation of free-surface fluctuations of liquid lithium flow for IFMIF lithium target by using an electro-contact probe, Fus. Eng. Des. 82 (2007) 2550–2557

[38] Wakai, E., et al., “Development of small specimen test techniques for the IFMIF test cell”, Proceedings of IAEA Fusion Energy Conference 2012, San Diego

[39] D. Rapisarda et al., “Study on the response of IFMIF fission chambers to mixed neutron-gamma fields: PH-2 experimental tests”, Fusion Eng. Des., 86 (2011) 1232

[40] Zinkle, S. et al., “Multimodal Options for materials research to advance the basis for fusion energy in the ITER era”, Proceedings of IAEA Fusion Energy Conference 2012, San Diego

[41] Fusion Electricity: A roadmap for the realisation of Fusion Energy, EFDA Nov 2012